Journal of Solid Mechanics Vol. 8, No. 2 (2016) pp. 232-246

Nonlocal Vibration of Y-SWCNT Conveying Fluid Considering a General Nonlocal Elastic Medium

A.H. Ghobanpour Arani [1], A. Rastgoo [1], A. Ghorbanpour Arani [2, 3 *], M. Sh. Zarei [2]

[1] *School of Mechanical Engineering, College of Engineering, University of Tehran, Tehran, Iran*
[2] *Faculty of Mechanical Engineering, University of Kashan, Kashan, Iran*
[3] *Institute of Nanoscience& Nanotechnology, University of Kashan, Kashan, Iran*

Received 17 January 2016; accepted 22 March 2016

ABSTRACT

In this paper, a nonlocal foundation model is proposed to analyze the vibration and instability of a Y-shaped single-walled carbon nanotube (Y-SWCNT) conveying fluid. In order to achieve more accurate results, fourth order beam theory is utilized to obtain strain-displacement relations. For the first time, a nonlocal model is presented based on nonlocal elasticity and the effects of nonlocal forces from adjacent and non-adjacent elements on deflection are considered. The Eringen's theory is utilized due to its capability to consider the size effect. Based on Hamilton's principle, motion equations as well as boundary conditions are derived and solved by means of hybrid analytical-numerical method. It is believed that the presented general foundation model offers an exact and effective new approach to investigate vibration characteristics of this kind of structures embedded in an elastic medium. The results of this investigation may provide a useful reference in controlling systems in nano-scale.

© 2016 IAU, Arak Branch.All rights reserved.

Keywords : Y-SWCNT; Nonlocal foundation model; Nonlocal elasticity theory; Fourth order beam theory; Hamilton's principle.

1 INTRODUCTION

A VARIETY of multi-terminal junctions of carbon nanotubes, including Y, T and X types were generated by connecting individual single-walled carbon nanotubes with different size and helicity[1], [2].Y-junction SWCNTs have a potential to utilize in the nano-scale three-terminal devices for controlling the switching, power gain or other transiting applications which are needed in a molecular electronic circuit[3], [4]. Y-junction SWCNTs are a novel structures composed of three terminals with different chiralities which is shown various electrical properties. The electrical characteristic of Y-SWCNTs provides insights to research into CNT networks (known as CNT mats) that are expected to have immediate application in nano-electro-mechanical system (NEMS) and sensors[5]. Carbon nanotube based electronics offers significant potential as a nano-scale alternative to silicon-based devices for molecular electronics technologies. The mutual interaction of the electron currents in the three branches of the Y-junction is shown to be the basis for a potentially new logic device. These nanotubes have been found to exhibit both electrical switching and logic behavior. Tiny tubes of carbon, crafted into the shape of a Y,could revolutionize the computer industry, suggests new research. The paper has shown that Y-shaped carbon nanotubes are easily made and act as remarkably efficient electronic transistors - the toggles used to control the flow of electrons through computer circuits.

*Corresponding author. Tel.: +98 31 55912450; Fax: +98 31 55912424.
E-mail address: aghorban@kashanu.ac.ir (A. Ghorbanpour Arani).

© 2016 IAU, Arak Branch. All rights reserved.

Through this paper, we are enabling and adding a new functionality to nanotube electronics that is, switching making an overall CNT-based nano-electronic architecture more complete and feasible. The detailed nature of the abrupt electrical switching behavior is not completely understood but can be a fertile ground for future research, for example, in defect engineering where one can intentionally modify, mechanically or chemically, the paths of electronic conduction in the Y-junction. The brief exceptional properties which are cited above show the complexity and interesting of this research. In this regard, some published papers done by researchers have been collected to review before introducing present work Biro et al. [6] presented a paper including available data about carbon nanotube Y junctions along with the structural models and the transport calculations on it. Also, they studied the different methods, which is successfully produced these junctions and the available experimental transport and tunneling data of the grown junctions. They analyzed the common features of the various growth methods and proposed particularities of branched nano-objects.

Recently, some experimental works are performed to investigate properties of Y-SWCNT. Bandaru et al.[4] observed an abrupt modulation of the current form an on-to an off-state, presumably mediated by defects and the topology of the junction. In this paper is shown that the mutual interaction of the electron currents in the three branches of the Y-junction to be the basis for a potentially new logic device. Choi and Choi [7] investigated the synthesis of a Y-junction SWCNTs and its electrical characterization. They found that the catalyst composition, which is related to the Gibbs free energy of metal carbide formation, is a significant parameter in formation of Y-junction branches. Based on MD simulation, Park et al. [8] showed the capability of Y-junction carbon nano-tube to separate K+ and Cl− ions from a KCl solution. Zhang et al. [9] researched on the piezoelectric pump with its Y-shape pipes. They obtained the relation between the frequencies of the piezoelectric vibrator and the mean pressure in the chamber and compared the theoretical results with experimental tests.

As mentioned, due to exceptional properties of carbon nanotube junction in nano devices, it has attracted a lot of scientists. In this regard, Filiz and Aydogdu [10] researched into axial vibration of carbon nanotube heterojunctions based on nonlocal theory. They found that the frequency of heterojunction is dependent upon length and cross section of each segment of CNTs.

In recent years, various researches have been carried out to analyzing the buckling, dynamic stability and free vibration of beams and CNTs embedded in elastic medium. In this regard, Avramidis and Morfidis [11] introduced Kerr-type three-parameter elastic foundation for bending analysis of a Timoshenko beam. They solved governing equations analytically and indicated that the Kerr-type three-parameter elastic foundation is much superior to one or two parameter models. Challamel et al. [12] employed nonlocal Reissner foundation model to study buckling of elastic beams. They found that size effect is an important parameter and nonlocal foundation model should be used to achieve more accurate results. Based on nonlocal elasticity theory Failla et al. [13] presented a two-dimensional foundation model that is of as an ensemble of soil column elements resting on an elastic base. A two-parameter elastic foundation for analysis of beam was presented by Shen[14]. He revealed that the foundation stiffness has a significant effect on the nonlinear behavior of Euler- Bernoulli beams.

Vibration and instability analysis of pipes and CNTs conveying fluid is conducted by many researches. Ghorbanpour Arani et al. [15] investigated the nonlinear nonlocal vibration and buckling of fluid-conveyed micro-tube reinforced by Boron-Nitride nanotubes (BNNTs) under electro-thermo-mechanical loadings embedded in an elastic medium. The effect of temperature on wave propagation in double-walled carbon nanotubes (DWCNTs) embedded in a polymer matrix was carried out by Besseghier et al.[16]. They used nonlocal elasticity theory and demonstrated that a temperature change is a key factor on transverse vibrations of DWCNT. Ghorbanpour Arani and Roudbari[17] studied the wave propagation of fluid- conveying single-walled Boron Nitride nanotubes (SWBNNTs) embedded in a vicsoelastic medium which is simulated as visco- Pasternak foundation by using Euler–Bernoulli beam (EBB) model. Ghorbanpour Arani et al. [18] presented the nonlinear vibration of DWCNTs embedded on Pasternak elastic medium and subjected to an axial fluid flow. Pak et al.[19]investigated vibrations of three dimensional angled pipe systems conveying fluid. They used Extended Hamilton's principle to derive motion equations and solved them by means of finite element method. They demonstrated that increasing the flow velocity leads to decrease the natural frequency of the system. This behavior can be seen especially as the geometry of the system is similar to the straight pipe.

In this paper, a novel approach is generalized to develop a corresponding nonlocal foundation. Based on this method, all of the elements have an important role to determine the displacement of elastic medium and the influences of nonlocal forces from adjacent and non-adjacent elements on deflection are also considered.

© 2016 IAU, Arak Branch

2 FORTH ORDER BEAM THEORY

Y-SWCNT consists of three separate CNTs which are jointed together at the end of first CNT. As shown in Fig.1, R_i and $L_i\ (i=1,2,3)$ denote the internal radius and length of CNTs. It's assumed that CNTs are connected together at the one junction point. In fact, it is considered that the continuity assumption is valid at the junction of CNTs. A triangle area in Figs.1 represents the two-dimensional area of junction point. In this paper, asymmetric Y-SWCNT has been considered in which α and β are the angle of second and third CNTs, respectively. Also, the coordinate system for each CNT has been considered, separately. It is worth to mention that z_1 axis is identical for three CNTs.

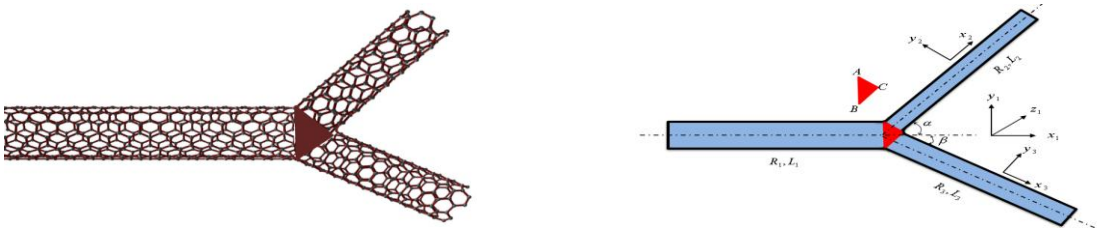

(a) (b)

Fig.1
(a) View of Y-SWCNTs (b) Simulation of Y-SWCNTS by three beams.

According to [20], in the fourth order beam theory it is assumed that the cross section is remained straight after applying loads. In the other word, the shear strain is negligible. The strain-displacement relationships are expressed as:

$$\begin{aligned}
&\tilde{U}(x,z,t)=u(x,t)-z\,\frac{\partial w(x,t)}{\partial x},\\
&\tilde{V}(x,z,t)=-z\,\phi(x,t),\\
&\tilde{W}(x,z,t)=w(x,t)+y\,\phi(x,t).
\end{aligned} \tag{1}$$

where x is the longitudinal coordinate, z is the coordinate measured from the mid-plane of the beam. The terms $u(x,t), v(x,t)$, and $w(x,t)$ are the longitudinal and transverse components of the displacement in the mid-plane of the beam, respectively. Also, $\varphi(x,t)$ denotes the torsional deformation of cross section.

3 THE EFFECT OF FLOW SEPARATION AT THE JUNCTION

Changing in motion direction of fluid at junction point causes to create forces. When the fluid reaches to the end of the first nanotube, it is divided into two parts. One part flows into second nanotube with α angle to the horizon in a clockwise direction and another part with β angle to the horizon in a counterclockwise direction flows into third nanotube.

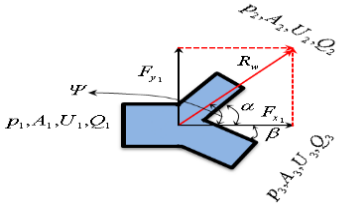

Fig.2
Created forces by divisions of fluid in Y-SWCNT.

At the junction point, the fluid velocity is not zero and the pressure is not high, so the forces due to change in

© 2016 IAU, Arak Branch

momentum are slowly distributed and forces equilibrium conditions are govern. So for control volume exhibited in Fig. 2, the applied forces on the main nanotube in x_1 and y_1 directions can be expressed as:

$$F_{x_1} = p_1A_1 - p_2A_2\cos\alpha - p_3A_3\cos\beta + \rho A_1U_1^2 - \rho A_2U_2^2\cos\alpha - \rho A_3U_3^2\cos\beta, \tag{2}$$

$$F_{y_1} = p_2A_2\sin\alpha + p_3A_3\sin\beta - \rho A_2U_2^2\sin\alpha - \rho A_3U_3^2\sin\beta. \tag{3}$$

Assuming no pressure drop at junction point and according to Bernoulli's equation, the fluid velocity of each nanotubes are equal at junction point; thus, the continuity equation is written as follows:

$$Q_1 = Q_2 + Q_3 \xrightarrow{U_1=U_2=U_3} A_1 = A_2 + A_3. \tag{4}$$

Using Eqs. (2) to (4) the resultant force caused by the change in fluid's momentum in the y junctions is follow:

$$\begin{aligned} R_w &= \left[F_{x_1}^2 + F_{y_1}^2\right]^{\frac{1}{2}} = (p_1A_1 + M^fU_1^2)\begin{bmatrix}(1-q\cos\alpha + q\cos\beta - \cos\beta)^2\\ +(-q\sin\alpha - q\sin\beta + \sin\beta)\end{bmatrix}^{\frac{1}{2}},\\ \psi &= \tan^{-1}\left[\frac{F_{y_1}}{F_{x_1}}\right] = \tan^{-1}\left[\frac{-q\sin\alpha - q\sin\beta + \sin\beta}{1-q\cos\alpha + q\cos\beta - \cos\beta}\right]. \end{aligned} \tag{5}$$

where $A_2/A_1 = q$. The tensile forces along the axial and transverse directions exert to the Y-SWCNT due to the fluid flow at the *Y*-junction can be obtain by writing force equilibrium equations in the x_2 and x_3 directions:

$$F_{x_2} = R_w\frac{\sin(\psi+\beta)}{\sin(\alpha-\beta)},\quad F_{x_3} = R_w\frac{\sin(\psi+\alpha)}{\sin(\alpha-\beta)} \tag{6}$$

4 INFLUENCES OF SLIP CONDITIONS ON THE VELOCITY PROFILE

For solving the problem of micro-nano-flows a dimensionless parameter Knudsen number (*Kn*) is defined and used to correcting the velocity profile of fluid. *Kn* may change from zero to infinitive value where zero value corresponds to Euler equations in which the variation of flow fluid is disregarded. Since the Navier-stokes equations are valid for $Kn < 0.01$, it is necessary to modify this equation for slip boundary conditions.

On the other hand, the slip boundary condition is considered for the fluid flow regime inside the nanotube and following assumption is considered:

- The fluid flow obeys the continuum mechanics (i.e. the fluid is continuous).
- The fluid is incompressible,
- The sliding layer thickness between the nanotube and fluid is assumed to be much close to zero.

In this regard, the profile of fluid velocity is amended to obtain the modified Navier-stokes equation which is valid in $10^{-2} < Kn < 10^{-1}$ as follows:

$$\frac{1}{\mu^e}\frac{dp}{dx} = \frac{\partial^2U(r)}{\partial r^2} + \frac{1}{r}\frac{\partial U(r)}{\partial r}. \tag{7}$$

Solving Navier-Stokes equation along the longitudinal direction yields the following fluid velocity distribution as:

$$U(r) = \frac{1}{4\mu_e}\left(\frac{\partial p}{\partial x}\right)r^2 + C_1\ln r + C_2, \tag{8}$$

© 2016 IAU, Arak Branch

where *r* is the radial distance from the center line of the nanotube, C_1 and C_2 are the integration constants. Since at the center line of the nanotube ($r=0$) the fluid velocity is limited, C_1 is equal to zero. The velocity profile is obtained by applying both slip and no-slip boundary conditions at the Y-SWCNT wall as follows:

$$U_{slip}=\frac{1}{4\mu_0\left(\frac{1}{1+aKn}\right)}\left(\frac{\partial p}{\partial x}\right)\left[r^2-R^2-2R^2\left(\frac{2-\sigma_v}{\sigma_v}\right)\left(\frac{Kn}{1+Kn}\right)\right],$$
$$U_{no-slip}=\frac{1}{4\mu_0}\left(\frac{\partial p}{\partial x}\right)\left(r^2-R^2\right), \tag{9}$$

The accommodation coefficient is considered as $\sigma_v=1$. The relationship between the bulk viscosity and effective viscosity is $\frac{\mu^o}{\mu^e}=[1+aKn]$ and $a=0.864\tan^{-1}(4Kn^{0.4})$ [21].

Considering velocity profiles obtained from Eqs. (9), the velocity correction factor γ can be defined as follows:

$$\gamma=\frac{U_{slip}}{U_{no-slip}}=\left(1+aKn\right)\left(4\left(\frac{2-\sigma_v}{\sigma_v}\right)\left(\frac{Kn}{Kn+1}\right)+1\right). \tag{10}$$

Therefore, the corrected velocity of fluid in the whole equations is considered with the form of $U=\gamma U_{no-slip}$.

5 NONLOCAL ELASTICITY THEORY

In this paper the nonlocal theory [20] is employed to deriving equations of motion. Unlike the Hooke's law, in nonlocal elasticity theory, the stress field at a reference point x depends on the strain at all other points in the body. The singularity of stress field near a dislocation core and a crack tip can be avoided by means of this theory. In addition, some phenomena related to atomic and molecular scale such as high frequency vibrations and wave dispersion can be justified in this proposed theory. Therefore, in the absent of body force, the constitutive equation includes stresses σ and strains ε tensors can be expressed as follows:

$$(1-\mu\nabla^2)\sigma_x^{nl}=\sigma_x^{l}=(\lambda+2G)(\frac{\partial u}{\partial x}-z\frac{\partial^2 w}{\partial x^2}), \tag{11a}$$

$$(1-\mu\nabla^2)\sigma_{xy}^{nl}=\sigma_{xy}^{l}=-Gz\frac{\partial \phi}{\partial x}, \tag{11b}$$

$$(1-\mu\nabla^2)\sigma_{xz}^{nl}=\sigma_{xz}^{l}=2G\varepsilon_{xz}=Gy\frac{\partial \phi}{\partial x}, \tag{11c}$$

where superscript *l* and *nl* denote the local and nonlocal parameters. $\mu=e_o a_o$ is the nonlocal parameter. The strain energy of an elastic body is expressed as:

$$U^{total}=\frac{1}{2}\int_0^L\left[N_x^{nl}\frac{\partial u}{\partial x}-M_y^{nl}\frac{\partial^2 w}{\partial x^2}+M_t^{nl}\frac{\partial \phi}{\partial x}\right]dx, \tag{12}$$

In which $N_x^{nl}=\int_{A^t}\sigma_x^{nl}dA^t$, $M_y^{nl}=\int_{A^t}z\,\sigma_x^{nl}dA^t$, $M_t^{nl}=\int_{A^t}[y\,\sigma_{xz}^{nl}-z\,\sigma_{xy}^{nl}]dA^t$.

© 2016 IAU, Arak Branch

The kinetic energy of CNT includes two discrete parts given as follows:

$$K^t = K^{bulk} + K^{fluid} = \frac{1}{2}\int_0^L \{(m^t + M^f)[(\frac{\partial u}{\partial t})^2 + (\frac{\partial w}{\partial t})^2] + (\rho^t I^t + \rho^f I^f)(\frac{\partial^2 w}{\partial t \partial x})^2 + (\rho^t J^t + \rho^f J^f)(\frac{\partial \phi}{\partial t})^2 + M^f U^2 + 2M^f U \frac{\partial u}{\partial t} + M^f U^2 (\frac{\partial w}{\partial x})^2 + 2M^f U \frac{\partial w}{\partial t}\frac{\partial w}{\partial x}\} dx . \quad (13)$$

Also, the boundary forces acting on the beginning and end of nanotube $(x = 0, x = L)$ must be considered as follows:

$$\delta\Omega^t = \int_0^L [(q_x^{B^f} + \bar{q}_{tx}^{B^t})\delta u + (q_z^J + q_z^{B^f} + \bar{q}_{tz}^{B^t} + q_z^m)\delta w]dx + \bar{N}_x \delta u \Big|_0^L + \bar{V}_z \delta w \Big|_0^L - \bar{M}_y \frac{\partial \delta w}{\partial x}\Big|_0^L + \bar{M}_t \delta\phi \Big|_0^L], \quad (14)$$

where $\delta\Omega^t$ is the virtual paper due to small displacement and $\bar{N}_x, \bar{V}_z, \bar{M}_y$ and $\bar{M}_t$ are the boundary forces and boundary momentums and q_z^J is change of fluid momentum force at junction point.

6 NONLOCAL FOUNDATION MODEL

In the present paper, the asymmetric Y-SWCNT is surrounded by elastic medium. The force applied on asymmetric Y-SWCNT due to elastic foundation is q^m and the motion equation in the transverse direction expressed as $F(x,t) + q^m = 0$ .In this model, all of the elements have an important role to determine the displacement of elastic medium. Fig. 3 shows the schematic of elastic medium with the force due to adjacent and non-adjacent for four elements.

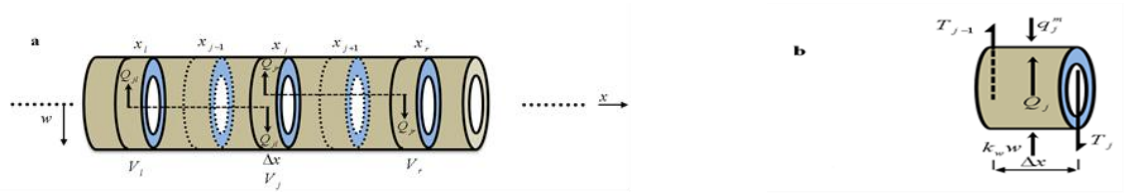

(a) (b)

Fig.3
(a) Schematic view of the nonlocal elastic medium (b) Vertical equilibrium of the proposed nonlocal elastic model.

The constitutive relation of the presented model of foundation interactions is obtained by vertical equilibrium of the layer element $V_j = A^m \Delta x$ at located $x_j = (j-1)\Delta x$,so $(j = -\infty, ..., -1, 0, 1, ..., \infty)$, Δx is size of each element and A^m is the cross section of elastic medium. In the nonlocal elastic model the foundation element is in equilibrium under the external load q_j^m ,the reaction of the local spring element $k_w \Delta x$, the contact shear forces T_{j-1} and T_j, the resultant of long-range forces exerted by surrounding volumes, on the left and on the right of volume V_j that follow as:

$$Q_j^L = \sum_{l=-\infty}^{j-1} Q_{jl}, \; Q_j^R = \sum_{l=j+1}^{\infty} Q_{jr} \quad (15)$$

where Q_{jl} and Q_{jr} are the differences forces between volume elements *j,l* and *j,r*.

© 2016 IAU, Arak Branch

In this context, the nonlocal interactions between elements *j,l* and *j,r* are expressed as follows:

$$Q_j^L = \sum_{l=-\infty}^{j-1} G(|x_j - x_l|)(w_j - w_l)\Delta x, \tag{16a}$$

$$Q_j^R = \sum_{r=j+1}^{\infty} G(|x_j - x_r|)(w_j - w_r)\Delta x. \tag{16b}$$

where $G(|x_j - x_l|)$ is the green function which is called nonlocal stiffness. Therefore, the force applied on the whole elements due to adjacent and non-adjacent can be written as:

$$Q_j = Q_j^L - Q_j^R \tag{17}$$

If $\Delta x \to 0$, the constitutive equation for the nonlocal foundation interactions is obtained in the integral form as follows:

$$Q = \int_0^L G(|x - x'|)(w(x) - w(x'))dx'. \tag{18}$$

Therefore, the equilibrium of forces on the whole domain can be written as:

$$q^m = k_w w + \int_0^L G(|x - x'|)(w(x) - w(x'))dx' - G_s \frac{\partial^2 w}{\partial x^2}. \tag{19}$$

where, the first term is related to the vertical force in Winkler model. The second term includes nonlocal force and third term is local shear force. The schematic of elastic medium with the force due to adjacent and non-adjacent for four elements is presented in Fig. 4.

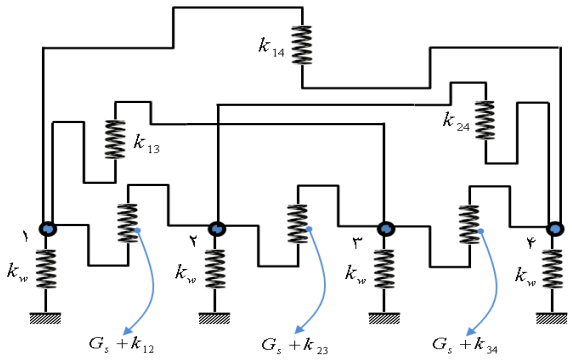

Fig.4
The schematic of elastic medium with the force due to adjacent and non-adjacent for four elements.

Based on Green function and applying nonlocal theory, the lateral motion equation can be determined:

$$F(x,t) - l_c^2 k_{nl} \frac{\partial^2 F(x,t)}{\partial x^2} - (l_c^2 k_{nl} k_o + G_s)\frac{\partial^2 w}{\partial x^2} + (k_w + k_{nl})w + l_c^2 k_{nl} G_s \frac{\partial^4 w}{\partial x^4} = 0, \tag{20}$$

where k_{nl} and l_c denote the nonlocal stiffness of medium and the internal length of each elements, respectively, and k_o is $k_o = k_w + 2k_{nl}$. As can be seen, when $l_c = k_{nl} = G_s = 0$ Winkler model is obtained and the Pasternak model is calculated when $l_c = k_{nl} = 0$ .Results reveal that present nonlocal elastic foundation model can be a general model so that it is included other models.

© 2016 IAU, Arak Branch

7 EQUATIONS OF MOTION

The equations of motion and boundary conditions can be derived by Hamilton's variational principle that can be formulated as [22]:

$$\delta\int_{t_1}^{t_2}\left[K-(U-\Omega)\right]dt=0. \tag{21}$$

Substituting Eqs. (12), (13) and (14) into Eq. (21) and setting the coefficients of δu_k , δw_k and $\delta\phi_k$ to zero and considering the linear terms leads to the following differential equation of motion for nonlocal elastic foundation as follows:

$$a_{1k}\frac{\partial^5\bar{u}_k}{\partial\tau\partial\bar{x}_k^4}+a_{2k}\frac{\partial^2\bar{u}_k}{\partial\bar{x}_k^2}+a_{3k}\frac{\partial^4\bar{u}_k}{\partial\tau^2\partial\bar{x}_k^2}+a_{4k}\frac{\partial^3\bar{u}_k}{\partial\tau\partial\bar{x}_k^2}+a_{5k}\frac{\partial^2\bar{u}_k}{\partial\tau^2}=0, \tag{22}$$

$$\begin{aligned}&-\bar{l}_c^2b_{1k}\frac{\partial^6\bar{w}_k}{\partial\bar{x}_k^6}-\bar{l}_c^2b_{2k}\frac{\partial^5\bar{w}_k}{\partial\bar{x}_k^5}+(b_{3k}-\bar{l}_c^2b_{4k})\frac{\partial^4\bar{w}_k}{\partial\bar{x}_k^4}-\bar{l}_c^2b_{6k}\frac{\partial^6\bar{w}_k}{\partial\tau^2\partial\bar{x}_k^4}+b_{2k}\frac{\partial^3\bar{w}_k}{\partial\bar{x}_k^3}-\bar{l}_c^2b_{7k}\frac{\partial^4\bar{w}_k}{\partial\tau\partial\bar{x}_k^3}\\&+(b_{6k}-\bar{l}_c^2b_{8k})\frac{\partial^4\bar{w}_k}{\partial\tau^2\partial\bar{x}_k^2}+b_{5k}\frac{\partial^2\bar{w}_k}{\partial\bar{x}_k^2}+b_{7k}\frac{\partial^2\bar{w}_k}{\partial\tau\partial\bar{x}_k}+b_{8k}\frac{\partial^2\bar{w}_k}{\partial\tau^2}+b_{9k}\bar{w}_k=0,\end{aligned} \tag{23}$$

$$c_{1k}\frac{\partial^2\bar{\phi}_k}{\partial\bar{x}_k^2}+c_{2k}\frac{\partial^4\bar{\phi}_k}{\partial\tau^2\partial\bar{x}_k^2}+c_{3k}\frac{\partial^2\bar{\phi}_k}{\partial\tau^2}=0. \tag{24}$$

Above equations developed to nine linear equations for $k=1,2,3$ where a_{nk} , b_{nk} and c_{nk} are cited in Appendix A. It is worth to mention that none of motion equations are coupled together, so the natural and geometric boundary conditions are obtained in order to create coupling among motion equations and maintain continuity condition which presented in Appendix B. It is convenient to introduce the following non-dimensional parameters for generality of the solution as:

$$\begin{aligned}&\bar{x}_k=\frac{x_k}{L_k},\bar{u}=\frac{u_k}{L_k},\bar{w}_k=\frac{w_k}{L_k},\bar{l}_k=\frac{l_k}{L_1},\bar{l}_{ck}=\frac{l_c}{L_1},e_k=\frac{L_k}{L_1},\tau=\frac{t}{L_1^2}\left[\frac{EI_1^t}{M_1^f+m_1^t}\right]^{\frac{1}{2}},\\&\bar{U}_k=L_1U_k\left[\frac{M_1^f}{EI_1^t}\right]^{\frac{1}{2}},d_k=\left[\frac{I_k^t}{I_1^t}\right]^{\frac{1}{2}},\beta_k=\left[\frac{M_k^f}{M_k^f+m_k^t}\right]^{\frac{1}{2}},\beta_{Tk}=\left[\frac{M_k^f+m_k^t}{M_1^f+m_1^t}\right]^{\frac{1}{2}},\\&\beta_{fk}=\frac{M_k^f}{\left[M_1^f(M_1^f+m_1^t)\right]^{\frac{1}{2}}},\bar{M}_k^f=\left[\frac{M_k^f}{M_1^f}\right]^{\frac{1}{2}},\gamma_k=\frac{(\lambda+2G)A_k^tL_k^2}{EI_k^t},\lambda_k=\frac{\lambda+2G}{E},\\&h_k=\frac{GA_k^tL_1^2}{EI_k^t},b_k=\frac{3L_1^2A_k^t}{J_k^t},\nu_k=\frac{EI_1^t}{GJ_k^t},r_k=\frac{J_k^tG}{EI_k^t},\bar{\mu}_k=\frac{\mu}{L_k^2},\sigma_k=\frac{\rho^tI_k^t+\rho^fI_k^f}{L_k^2(M_k^f+m_k^t)},\\&\kappa_k=\frac{\rho^tJ_k^t+\rho^fJ_k^f}{L_k^2(M_k^f+m_k^t)},S_k=\frac{I_k^t}{A_k^tL_k^2},\bar{\mu}_k^e=\frac{\mu_k^eA_k^f}{\left[EI_k^tM_k^f\right]^{\frac{1}{2}}},\bar{q}_k^J=\frac{q_{xk}^JL_k^2}{EI_k^t}.\end{aligned} \tag{25}$$

© 2016 IAU, Arak Branch

8 NUMERICAL SOLUTIONS

In order to solve motion equations, following functions are defined to separate time and space variables:

$$\begin{aligned}
&\bar{u}_k(\bar{x}_k,\tau)=\tilde{u}_k(\bar{x}_k)e^{i\omega\tau},\\
&\bar{w}_k(\bar{x}_k,\tau)=\tilde{w}_k(\bar{x}_k)e^{i\omega\tau},\\
&\bar{\phi}_k(\bar{x}_k,\tau)=\tilde{\phi}_k(\bar{x}_k)e^{i\omega\tau},
\end{aligned} \tag{26}$$

where ω is non-dimensional frequency which is introduced in form of $\omega=\left[\dfrac{M_1^f+m_1^t}{EI_1^t}\right]^{\frac{1}{2}}L_1^2\Omega$ that Ω is circular frequency. By considering above relations the time variable is omitted in the governing equations. Therefore, the equations of motion can be written as:

$$\bar{a}_{1k}\frac{\partial^4\bar{u}_k}{\partial\bar{x}_k^4}+\bar{a}_{2k}\frac{\partial^2\bar{u}_k}{\partial\bar{x}_k^2}+\bar{a}_{3k}\bar{u}_k=0, \tag{27}$$

$$\bar{b}_{1k}\frac{\partial^6\bar{w}_k}{\partial\bar{x}_k^6}+\bar{b}_{2k}\frac{\partial^5\bar{w}_k}{\partial\bar{x}_k^5}+\bar{b}_{3k}\frac{\partial^4\bar{w}_k}{\partial\bar{x}_k^4}+\bar{b}_{4k}\frac{\partial^3\bar{w}_k}{\partial\bar{x}_k^3}+\bar{b}_{5k}\frac{\partial^2\bar{w}_k}{\partial\bar{x}_k^2}+\bar{b}_{6k}\frac{\partial\bar{w}_k}{\partial\bar{x}_k}+\bar{b}_{7k}\bar{w}_k=0, \tag{28}$$

$$\bar{c}_{1k}\frac{\partial^2\bar{\phi}_k}{\partial\bar{x}_k^2}+\bar{c}_{2k}\bar{\phi}_k=0. \tag{29}$$

where $\bar{a}_{nk}$,$\bar{b}_{nk}$ and $\bar{c}_{nk}$ are cited in Appendix B. For the sake of the brevity of this paper, boundary conditions aren not mentioned here.

The solutions of Eqs. (27) to (29) are assumed as the following forms:

$$\begin{aligned}
&\tilde{u}_k(\bar{x}_k)=\sum_{n=1}^{L}\tilde{u}_{nk}e^{ip_{nk}\bar{x}_k},\\
&\tilde{w}_k(\bar{x}_k)=\sum_{n=1}^{M}\tilde{w}_{nk}e^{is_{nk}\bar{x}_k},\\
&\tilde{\phi}_k(\bar{x}_k)=\sum_{n=1}^{N}\tilde{\phi}_{nk}e^{ir_{nk}\bar{x}_k}.
\end{aligned} \tag{30}$$

Based on the order of differential Eqs. (30), $L=4, M=6$ and $N=2$ are selected. In addition, $p_{nk}(\omega), s_{nk}(\omega)$ and $r_{nk}(\omega)$ are the roots of characteristic equation. $\tilde{u}_{nk}$,$\tilde{w}_{nk}$ and $\tilde{\phi}_{nk}$ are constants that obtained by boundary conditions which generate a 36th order matrix as follows:

$$\left[D_{ij}\right]\{\bar{d}\}=\{0\},\quad (i,j=1,2,...,36), \tag{31}$$

where:

$$\begin{aligned}
\{\bar{d}\}=\{&\tilde{u}_{11},\tilde{u}_{21},\tilde{u}_{31},\tilde{u}_{41},\tilde{w}_{11},\tilde{w}_{21},\tilde{w}_{31},\tilde{w}_{41},\tilde{w}_{51},\tilde{w}_{61},\tilde{\phi}_{11},\tilde{\phi}_{21},\tilde{u}_{12},\tilde{u}_{22},\tilde{u}_{32},\tilde{u}_{42},\tilde{w}_{12},\tilde{w}_{22},\tilde{w}_{32},\tilde{w}_{42},\tilde{w}_{52},\\
&\tilde{w}_{62},\tilde{\phi}_{12},\tilde{\phi}_{22},\tilde{u}_{13},\tilde{u}_{23},\tilde{u}_{33},\tilde{u}_{43},\tilde{w}_{13},\tilde{w}_{23},\tilde{w}_{33},\tilde{w}_{43},\tilde{w}_{53},\tilde{w}_{63},\tilde{\phi}_{13},\tilde{\phi}_{23}\}^T.
\end{aligned} \tag{32}$$

© 2016 IAU, Arak Branch

In order to calculate frequencies of system, it is enough to solve following matrix relation:

$$\left(\det\left|D_{ij}\right|=0\right). \tag{33}$$

It is should be noted that the presented method in this study is adopted from [23]. For the sake of the brevity of this paper, Here the references are made to already mentioned ones for more clarity.

9 RESULTS AND DISCUSSION

In nanostructures like Y-SWCNTs, the small scale becomes significant and the nonlocal continuum model must be used to consider small scale effects in the motion equation, boundary conditions and forces between atoms and internal length scale in the construction of equations generated by the elastic foundation. Therefore, the equilibrium of each element is achieved due to a local reaction force, to contact forces exerted by the adjacent elements, nonlocal forces exerted by non-adjacent elements so that the local reaction force is simulated as in the Winkler and Pasternak models.

The analysis of frequency and critical fluid velocity of Y-SWCNT conveying fluid embedded in a general nonlocal elastic medium includes Winkler and Pasternak foundation are investigated in this paper. The geometrical and mechanical properties of Y-SWCNT are presented in Table 1.

Table1
The geometrical and mechanical properties of Y-SWCNT.

The geometrical and mechanical properties of Y-SWCNT [24]						
$E=1TPa$	$R_1=3.4nm$	$L_2=0.6L_1$	$L_3=0.8L_1$	$h_t=0.34nm$	$\beta_1=0.5$	$q=1/2$

Fig. 5 shows the variation of dimensionless frequency versus fluid velocity for different nonlocal or small scale parameters. It is evident from this figure that the value of dimensionless frequency is maximum for local vibration (i.e. $e_o a=0$). With increasing small scale parameter, the dimensionless frequency decreases and the rate of this reducing grows at higher nonlocal parameters. Accordingly, it can be said that Y-SWCNT have very high detection sensitivity so that the frequency of oscillation can be increased due to molecular adsorption, therefore the difference between the top and bottom of non-dimensional frequencies can help to identify different molecules.

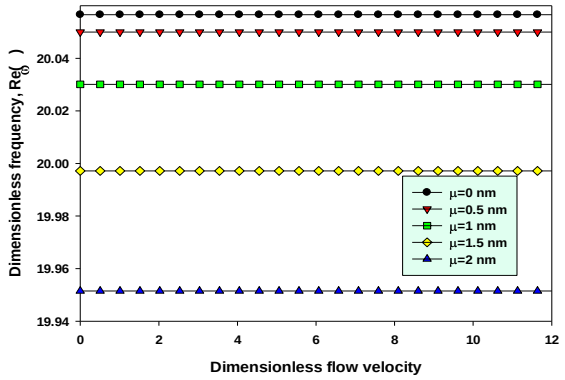

Fig.5
Effect of nonlocal parameter on vibration frequency of conveying Y-SWCNT at $\alpha=\beta=90^\circ$ $L_2=0.6L_1, L_3=0.8L_1$ $q=\frac{1}{2}$.

In Fig. 6, the result of present paper which is done by forth order beam theory has been compared with both Euler-Bernoulli and Rayleigh theories. The beam theory can be used to analyze of nanotubes when aspect ratio $(d/L>5)$. From this figure can be found that the difference between the obtain result from Euler-Bernoulli and Rayleigh beam theories is considerable in zero flow velocity. Due to negligible effect of rotational inertia of the fluid in comparison with centrifugal force, the results of both theories are converged with increasing fluid velocity. Fig. 6 shows that the percent difference of result for Euler-Bernoulli and Rayleigh theories by present work are 21.37% and 17.45%, respectively.

© 2016 IAU, Arak Branch

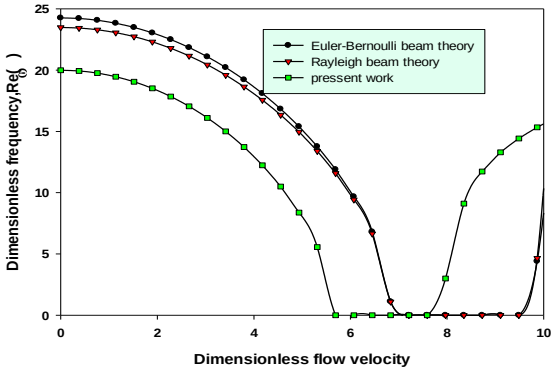

Fig.6
Comparison the results using three models.

Fig. 7 displays the effect of separation angle on the stability of Y-SWCNT conveying fluid. As can be seen, by increasing α and β the critical flow velocity increases which cause to more stable system. It is found that the fluid-conveying Y-SWCNT is always stable for $\alpha = \beta = 90^{\circ}$ or T-shaped case. Also, increasing α and β lead to increase growth rate of fluid critical velocity.

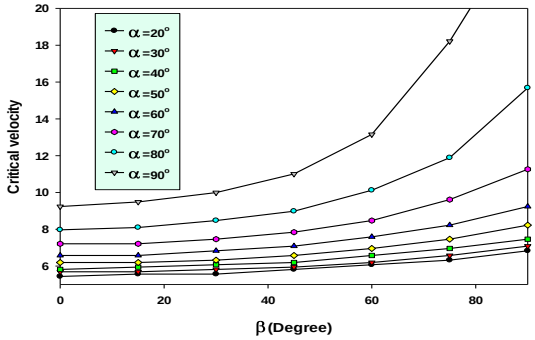

Fig.7
Effect of fluid separation angle on dimensionless frequency of conveying Y-SWCNT at $L_2 = 0.6L_1, L_3 = 0.8L_1$.

In this paper a general nonlocal elastic foundation is investigated. Fig. 8 describes the effect of this model on stability of system. Figs. 8(a) and 8(b) show the effect of spring constant on imaginary and real parts of frequency, respectively. These figures demonstrate that with increasing spring constant $\bar{k}_{nl}$ the stiffness and stability of system increases. It is concluded that in the nonlocal model the stability of Y-SWCNT is stiffer than local model (Winkler type).

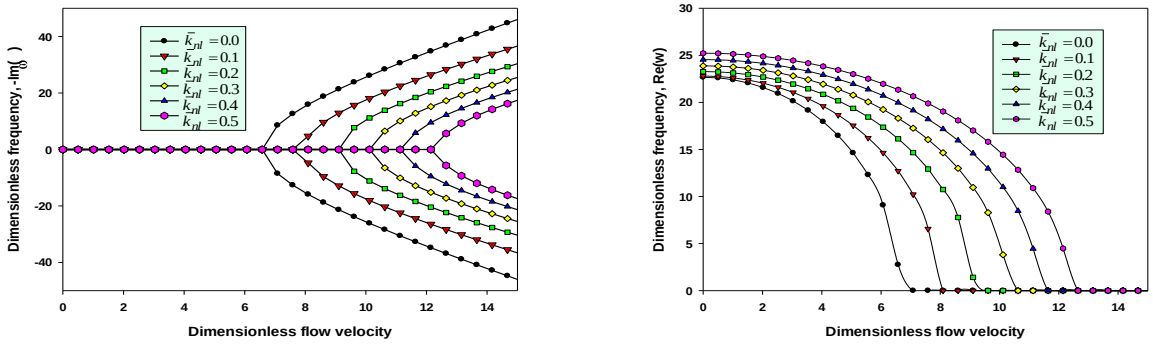

(a) (b)

Fig.8
Influence of spring coefficient of the nonlocal elastic model on the vibration frequency and system stability (a) damping frequency (b) vibration of frequency.

© 2016 IAU, Arak Branch

The comparison between the results of local and nonlocal elastic models is shown in Fig. 9. Fig. 9(a) and 9(b) present the damping and oscillation parts of frequency versus flow velocity for different internal length parameters. As can be observed, the stiffness and stability of nonlocal elastic model ($\bar{l}_c \neq 0$) is higher than local elastic model ($\bar{l}_c = 0$). In addition, dimensionless critical velocity for local model is 6.83 which increased with increasing internal length parameter.

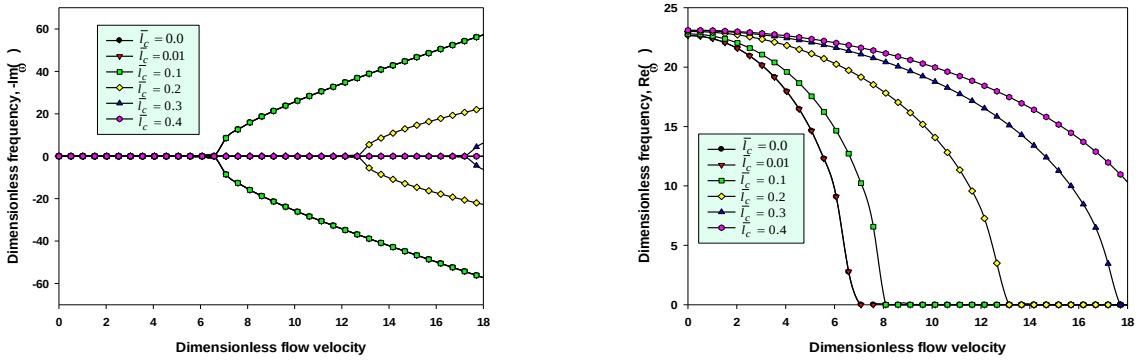

Fig.9
Influence of the characteristic length of the nonlocal elastic model on the vibration frequency and system stability (a) damping frequency (b) vibration of frequency.

Dimensionless natural frequencies with respect to dimensionless average flow velocity for different Knudsen numbers are plotted in Fig. 10. It can be found that the dimensionless critical average flow velocities of the system decreases with increasing Knudsen number in both first and second modes. Also it is seen from Fig. 10 that the dimensionless natural frequency is decreased as the Knudsen number is increased. Hence, the frequency is significantly influenced by the Knudsen number and the small-size effects of the flow field on the stability characteristics of the nanotubes cannot be ignored.

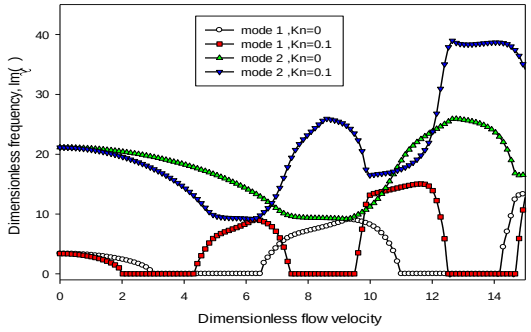

Fig.10
Influence of Knudsen number on the vibration frequency and system stability in two modes.

10 CONCLUSIONS

In this paper, a general nonlocal foundation model include Winkler and Pasternak elastic models was proposed and used to analyze the vibration and instability of a Y-SWCNT conveying fluid. It was assumed that the fluid is incompressible and irrotational and the fluid continuous equation with considering the slip boundary condition on the nanotube wall is used to obtain the velocity profile while the pressure at the junction is zero. Fourth order beam theory was employed to obtain strain-displacement relations where the Y-junction SWCNT is continuous and the nonlinear deformations are ignored. The effects of nonlocal forces from adjacent and non-adjacent elements on deflection were also considered. Utilizing Hamilton's principle, motion equations as well as boundary conditions were derived and solved by means of hybrid analytical-numerical method. Considering local and nonlocal foundation models, the influences of various parameters on vibration characteristics of Y-SWCNT conveying fluid

© 2016 IAU, Arak Branch

were discussed in details. Results revealed that increasing small scale parameter leads to decrease dimensionless frequencies. Moreover, the fluid conveying Y-SWCNT was always stable for $\alpha = \beta = 90^{\circ}$ or T-shaped case. It has been concluded that the stiffness and stability of nonlocal elastic model ($\bar{l}_c \neq 0, \bar{k}_{nl} \neq 0$) was higher than local elastic model ($\bar{l}_c = 0, \bar{k}_{nl} = 0$). Results of this investigation can be used in controlling systems such as power gain, or other transiting applications in nano-scale.

ACKNOWLEDGEMENTS

The authors are grateful to University of Kashan for supporting this paper by Grant No. 363443/67. They would also like to thank the Iranian Nanotechnology Development Committee for their financial support.

APPENDIX A

$$a_{1k} = \bar{\mu}_k \bar{\mu}_k^e \beta_k \beta_{Tk} e_k^2, a_{2k} = -\gamma_k d_k, a_{3k} = -\frac{\bar{\mu}_k \beta_{Tk}^2 e_k^2}{d_k}, a_{4k} = -\bar{\mu}_k^e \beta_k \beta_{Tk} e_k^2, a_{5k} = \frac{\beta_{Tk}^2 e_k^4}{d_k}, \tag{A.1}$$

$$\begin{aligned} &b_{1k} = d_k \lambda_k, b_{2k} = -\bar{U}_k \bar{M}_k^f e_k \bar{\mu}_k^e, b_{3k} = d_k [\lambda_k + \bar{l}_c^2 \bar{G}_{sk}], \\ &b_{4k} = -[-\frac{\bar{U}_k^2 \bar{M}_k^{f\,2} e_k^2}{d_k^2} + \bar{q}_k^J] d_k, b_{5k} = -[-\frac{\bar{U}_k^2 \bar{M}_k^{f\,2} e_k^2}{d_k^2} + \bar{q}_k^J - \bar{l}_c^2 \bar{k}_{ok} + \bar{G}_{sk}] d_k, \\ &b_{6k} = -\frac{\beta_{Tk}^2 e_k^4}{d_k} \sigma_k, b_{7k} = \frac{2\bar{U}_k \bar{M}_k^f \beta_k \beta_{Fk} e_k^3}{d_k}, b_{8k} = \frac{\beta_{Tk}^2 e_k^4}{d_k}, b_{9k} = [\bar{k}_{ok} - \bar{k}_{nlk}] d_k, \end{aligned} \tag{A.2}$$

$$c_{1k} = -d_k r_k, c_{2k} = -\frac{\bar{\mu}_k \kappa_k e_k^4}{d_k}, c_{3k} = \frac{\kappa_k e_k^4}{d_k}. \tag{A.3}$$

APPENDIX B

$$\bar{u}_k \Big|_{\substack{\bar{x}_k = 0 \\ k = 1,2,3}} = 0, \quad \bar{w}_k \Big|_{\substack{\bar{x}_k = 0 \\ k = 1,2,3}} = 0, \quad \bar{\phi}_k \Big|_{\substack{\bar{x}_k = 0 \\ k = 1,2,3}} = 0, \tag{B.1}$$

$$[\bar{d}_{1k} \frac{\partial^2 \bar{w}_k}{\partial \bar{x}_k^2} + \bar{d}_{2k} \frac{\partial^2 \bar{w}_k}{\partial \tau^2}] \Big|_{\substack{\bar{x}_k = 0 \\ k = 1,2,3}} = 0, \tag{B.2}$$

$$-\bar{d}_{2k} \frac{\partial \bar{u}_k}{\partial \bar{x}_k} \Big|_{\substack{\bar{x}_k = 1 \\ k = 1}} + \bar{d}_{2k} \frac{\partial \bar{u}_k}{\partial \bar{x}_k} \Big|_{\substack{\bar{x}_k = 1 \\ k = 2}} \cos\alpha + \bar{d}_{2k} \frac{\partial \bar{u}_k}{\partial \bar{x}_k} \Big|_{\substack{\bar{x}_k = 1 \\ k = 3}} \cos\beta = 0, \tag{B.3}$$

$$\sum_{k=1}^{3} [\bar{d}_{2k} \frac{\partial^6 \bar{w}_k}{\partial \tau^2 \partial \bar{x}_k^4} + \bar{d}_{4k} \frac{\partial^4 \bar{w}_k}{\partial \bar{x}_k^4} + \bar{d}_{5k} \frac{\partial^4 \bar{w}_k}{\partial \tau^2 \partial \bar{x}_k^2} + \bar{d}_{6k} \frac{\partial^2 \bar{w}_k}{\partial \bar{x}_k^2}] \Big|_{\bar{x}_k = 1} = 0, \tag{B.4}$$

$$\begin{aligned} &[\bar{d}_{1k} \frac{\partial^2 \bar{w}_k}{\partial \bar{x}_k^2} + \bar{d}_{2k} \frac{\partial^2 \bar{w}_k}{\partial \tau^2}] \Big|_{\substack{\bar{x}_k = 1 \\ k = 1}} - [\bar{d}_{1k} \frac{\partial^2 \bar{w}_k}{\partial \bar{x}_k^2} + \bar{d}_{2k} \frac{\partial^2 \bar{w}_k}{\partial \tau^2}] \Big|_{\substack{\bar{x}_k = 1 \\ k = 2}} \cos\alpha \\ &-[\bar{d}_{1k} \frac{\partial^2 \bar{w}_k}{\partial \bar{x}_k^2} + \bar{d}_{2k} \frac{\partial^2 \bar{w}_k}{\partial \tau^2}] \Big|_{\substack{\bar{x}_k = 1 \\ k = 3}} \cos\beta - [\bar{d}_{7k} \frac{\partial \bar{\phi}_k}{\partial \bar{x}_k}] \Big|_{\substack{\bar{x}_k = 1 \\ k = 2}} \sin\alpha + [\bar{d}_{7k} \frac{\partial \bar{\phi}_k}{\partial \bar{x}_k}] \Big|_{\substack{\bar{x}_k = 1 \\ k = 3}} \sin\beta = 0, \end{aligned} \tag{B.5}$$

© 2016 IAU, Arak Branch

$$[\bar{d}_{7k}\ \frac{\partial\bar{\phi}_k}{\partial\bar{x}_k}]\Big|_{k=1}^{\bar{x}_k=1} - [\bar{d}_{7k}\ \frac{\partial\bar{\phi}_k}{\partial\bar{x}_k}]\Big|_{k=2}^{\bar{x}_k=1}\cos\alpha - [\bar{d}_{7k}\ \frac{\partial\bar{\phi}_k}{\partial\bar{x}_k}]\Big|_{k=3}^{\bar{x}_k=1}\cos\beta$$
$$+[\bar{d}_{1k}\ \frac{\partial^2\bar{w}_k}{\partial\bar{x}_k^2} + \bar{d}_{2k}\ \frac{\partial^2\bar{w}_k}{\partial\tau^2}]\Big|_{k=2}^{\bar{x}_k=1}\sin\alpha - [\bar{d}_{1k}\ \frac{\partial^2\bar{w}_k}{\partial\bar{x}_k^2} + \bar{d}_{2k}\ \frac{\partial^2\bar{w}_k}{\partial\tau^2}]\Big|_{k=3}^{\bar{x}_k=1}\sin\beta = 0, \tag{B.6}$$

$$\frac{\partial\bar{\bar{w}}_k}{\partial\bar{x}_k}\Big|_0^{L_k} = 0,\ \textit{higher order condition}\ (z\ \textit{direction}) \tag{B.7}$$

$$\frac{\partial\bar{\bar{u}}_k}{\partial\bar{x}_k}\Big|_0^{L_k} = 0,\ \textit{higher order condition}\ (x\ \textit{direction}) \tag{B.8}$$

$$u_k\,|_{\,k=1} = u_k\,|_{\,k=2}\cos\alpha, \tag{B.9}$$

$$u_k\,|_{\,k=1} = u_k\,|_{\,k=3}\cos\beta, \tag{B.10}$$

$$w_k\,|_{k=1} = w_k\,|_{k=2}, \tag{B.11}$$

$$w_k\,|_{k=1} = w_k\,|_{k=3}, \tag{B.12}$$

$$\frac{\partial w_k}{\partial x_k}|_{k=1} = \frac{\partial w_k}{\partial x_k}\cos\alpha + \phi_k\ \sin\alpha\big|_{k=2}, \tag{B.13}$$

$$\frac{\partial w_k}{\partial x_k}|_{k=1} = \frac{\partial w_k}{\partial x_k}\cos\beta + \phi_k\ \sin\beta\big|_{k=3}, \tag{B.14}$$

$$\phi_k\,|_{k=1} = \phi_k\ \cos\alpha - \frac{\partial w_k}{\partial x_k}\sin\alpha\big|_{k=2}, \tag{B.15}$$

$$\phi_k\,|_{k=1} = \phi_k\ \cos\beta - \frac{\partial w_k}{\partial x_k}\sin\beta\big|_{k=3}. \tag{B.16}$$

$$\bar{d}_{1k} = d_k\lambda_k, \bar{d}_{2k} = d_k, \bar{d}_{3k} = \frac{\bar{\mu}_k\sigma_k\beta_{Tk}^2 e_k^4}{d_k},\ \bar{d}_{4k} = [\bar{\mu}_k d_k \bar{U}_k^2 \bar{M}_k^{f\,2} e_k^2 - \lambda_k d_k + \bar{\mu}_k d_k \bar{q}_k^J],$$
$$\bar{d}_{5k} = \frac{\beta_{Tk}^2 e_k^4}{d_k}\sigma_k, \bar{d}_{6k} = [\frac{\bar{U}_k^2 \bar{M}_k^{f\,2} e_k^2}{d_k} - d_k\bar{q}_k^J],\ \bar{d}_{7k} = d_k r_k. \tag{B.17}$$

REFERENCES

[1] Terrones M., Banhart F., Grobert N., Charlier J.C., Terrones H., Ajayan P., 2002, Molecular junctions by joining single-walled carbon nanotubes, *Physical Review Letters* **89**: 075505.

[2] Andriotis A., Menon M., Srivastava D., Chernozatonskii L., 2001, Rectification properties of carbon nanotube Y-junctions, *Physical Review Letters* **87**: 066802.

[3] Papadopoulos C., Rakitin A, Li J., Vedeneev A., Xu J., 2000, Electronic transport in Y-junction carbon nanotubes, *Physical Review Letters* **85**(16): 3476.

[4] Bandaru P., Daraio C., Jin S., Rao A., 2005, Novel electrical switching behaviour and logic in carbon nanotube Y-junctions, *Nature Materials* **4**: 663-668.

© 2016 IAU, Arak Branch

[5] Sattler K. D., *2010, Handbook of Nanophysics: Nanotubes and Nanowires*, CRC press.
[6] Biró L. P., Horváth Z. E., Márk G. I., Osváth Z., A.A. Koós , Benito A. M., Maser W., Lambin P., 2004, Carbon nanotube Y- junctions: growth and properties, *Diamond and Related Materials* **13**: 241-249.
[7] Choi Y. C.,Choi W., 2005, Synthesis of Y-junction single-wall carbon nanotubes, *Carbon* **43**: 2737-2741.
[8] Park J. H., Sinnott S. B., Aluru N. R., 2006, Ion separation using a Y-junction carbon nanotube, *Nanotechnology* **17**: 895-900.
[9] Zhang J., Lu J., Xia Q., 2007, Research on the valveless piezoelectric pump with Y-shape pipes, *Frontiers of Mechanical Engineering in China* **2**: 144-151.
[10] Filiz S., Aydogdu M., 2010, Axial vibration of carbon nanotube heterojunctions using nonlocal elasticity, *Computational Materials Science* **49**: 619-627.
[11] Avramidis I. E., Morfidis K., 2006, Bending of beams on three-parameter elastic foundation, *International Journal of Solids and Structures* **43**: 357-375.
[12] Challamel N., Meftah S. A., Bernard F., 2010, Buckling of elastic beams on nonlocal foundation: a revisiting of reissner model, *Mechanics Research Communications* **37**: 472-475.
[13] Failla G., Santini A., Zingales M., 2012, A nonlocal two-dimensional foundation model, *Archive of Applied Mechanics* **83**: 253-272.
[14] Shen H. S., 2011, A novel technique for nonlinear analysis of beams on two-parameter elastic foundations, *International Journal of Structural Stability and Dynamics* **11**: 999-1014.
[15] Ghorbanpour Arani A., Shajari A. R., Amir S., Loghman A., 2012, Electro-thermo-mechanical nonlinear nonlocal vibration and instability of embedded micro-tube reinforced by BNNT, conveying fluid, *Physica E: Low-Dimensional Systems and Nanostructures* **45**: 109-121.
[16] Besseghier A., Tounsi A., Houari M. S. A., Benzair A., Boumia L., Heireche H., 2011, Thermal effect on wave propagation in double-walled carbon nanotubes embedded in a polymer matrix using nonlocal elasticity, *Physica E: Low-Dimensional Systems and Nanostructures* **43**: 1379-1386.
[17] Ghorbanpour Arani A., Roudbari M. A., 2014, Surface stress, initial stress and knudsen-dependent flow velocity effects on the electro-thermo nonlocal wave propagation of SWBNNTs, *Physica B: Condensed Matter* **452**: 159-165.
[18] Ghorbanpour Arani A., Zarei M. S., Amir S., Khoddami Maraghi Z., 2013, Nonlinear nonlocal vibration of embedded DWCNT conveying fluid using shell model, *Physica B: Condensed Matter* **410**: 188-196.
[19] Pak C. H., Hong S.C. S., Yun Y. S. Y., 1991, On the vibrations of three-dimensional angled piping systems conveying fluid, *KSME Journal* **5**: 86-92.
[20] Eringen A. C., *2002, Nonlocal Continuum Field Theories*, Springer.
[21] Kaviani F., Mirdamadi H.R., 2012, Influence of knudsen number on fluid viscosity for analysis of divergence in fluid conveying nano-tubes, *Computational Materials Science* **61**: 270-277.
[22] Khodami Maraghi Z.,Ghorbanpour Arani A., Kolahchi R., Amir S., Bagheri M. R., 2013, Nonlocal vibration and instability of embedded DWBNNT conveying viscose fluid, *Composites Part B: Engineering* **45**: 423-432.
[23] Gregory R.W., Paidoussis M. P., 1966, Unstable oscillation of tubular cantilevers conveying fluid.I.theoy, *Proceedings of the Royal Society of London, Series A, Mathematical and Physical Sciences* **293**: 512-527.
[24] Zhen Y., Fang B., 2010, Thermal-mechanical and nonlocal elastic vibration of single-walled carbon nanotubes conveying fluid, *Computational Materials Science* **49**: 276-282.

© 2016 IAU, Arak Branch